

The Heliospheric Ambipolar Potential Inferred from Sunward- Propagating Halo Electrons

Konstantinos Horaites

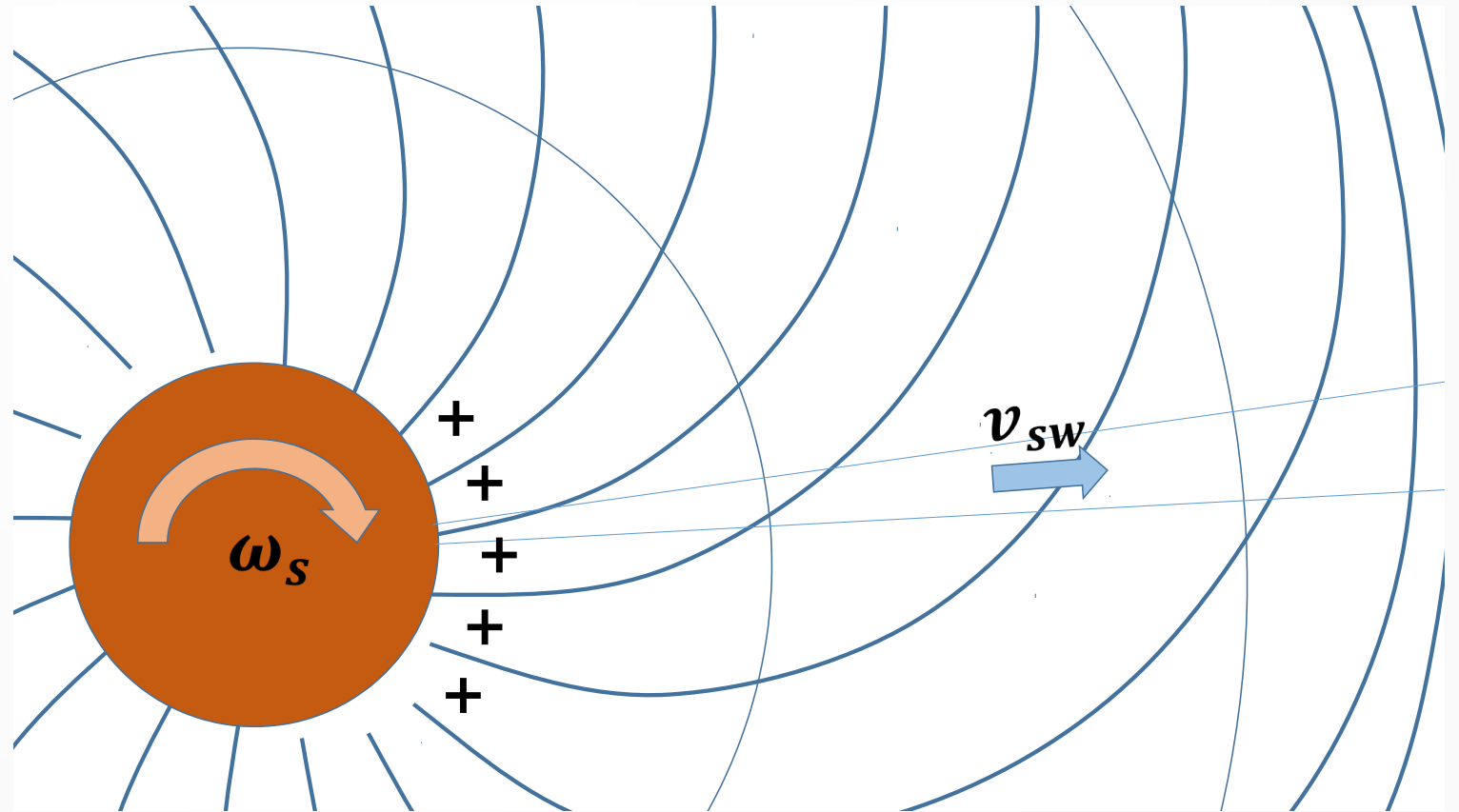
University of Helsinki

Stanislav Boldyrev

University of Wisconsin-Madison

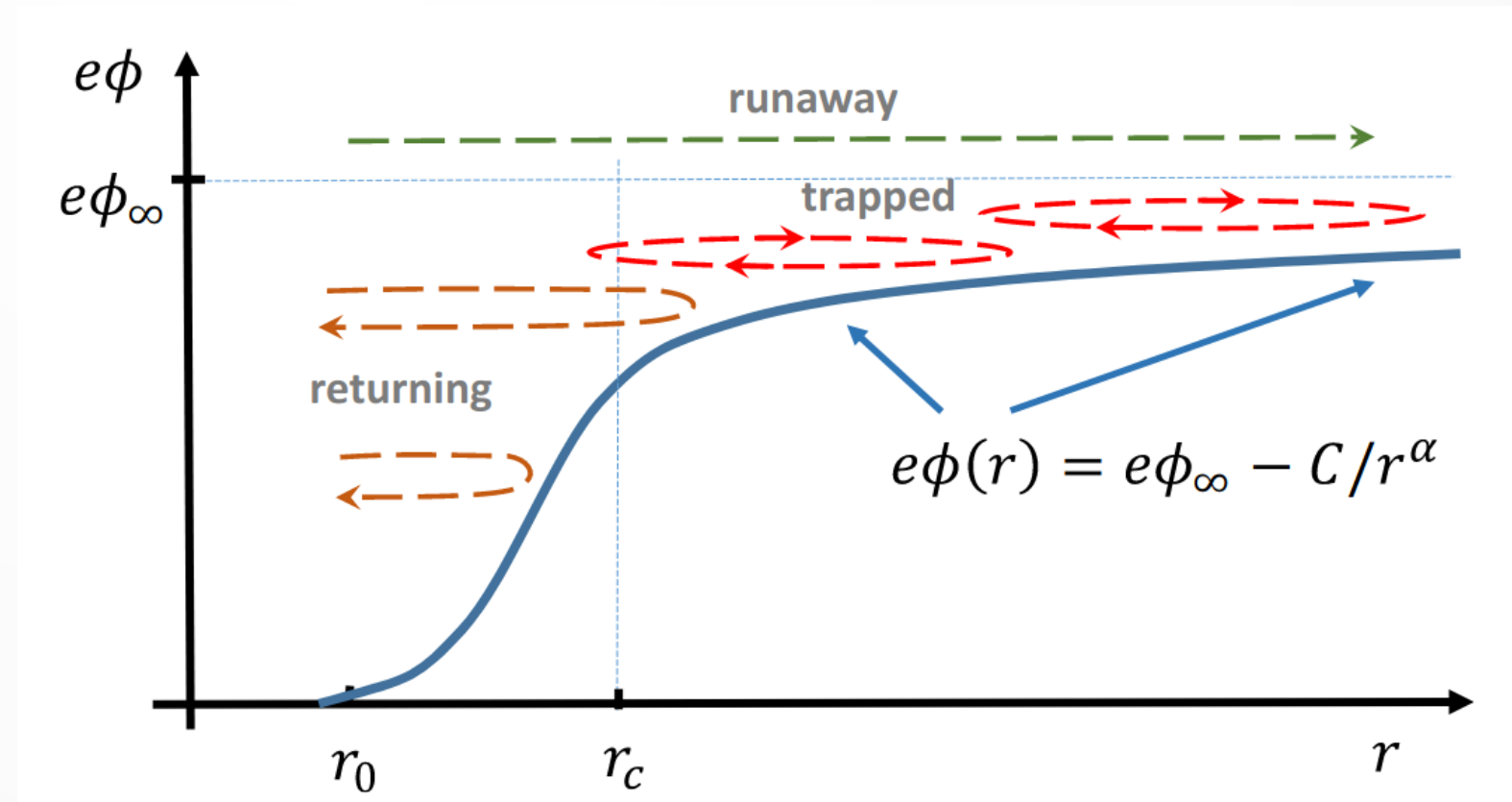
Ambipolar Potential

- Electrons (lower mass) tend to escape corona faster than protons
- A net positive charge is left behind
- In equilibrium, an electrostatic potential is established



Ambipolar Potential

- Ambipolar potential forms **trapped** and **runaway** electron populations.
- The trapped population is bound by two processes:
 - Electrostatic reflection (at large r)
 - Magnetic mirroring (at small r)



Boldyrev et al., (2020)

Electron VDFs

- Core (trapped)
- Halo
- Strahl (runaway)

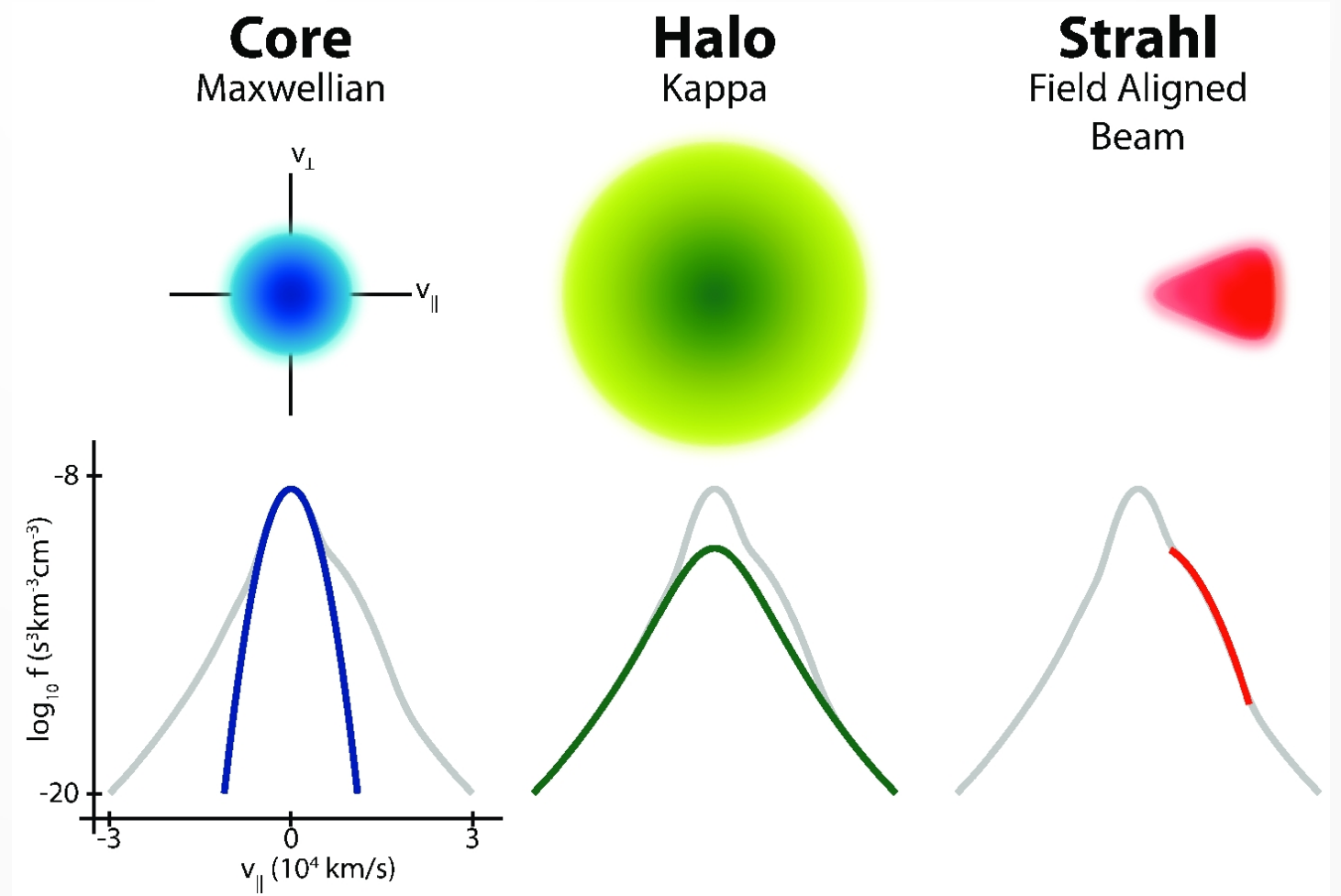
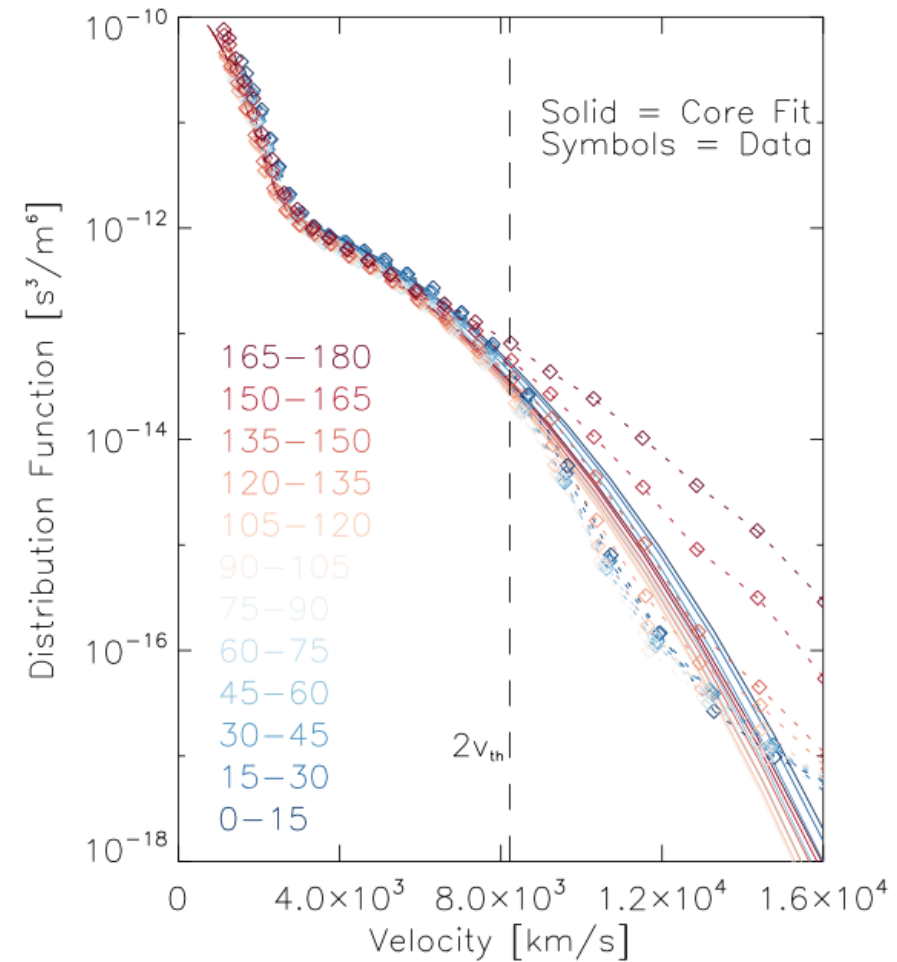
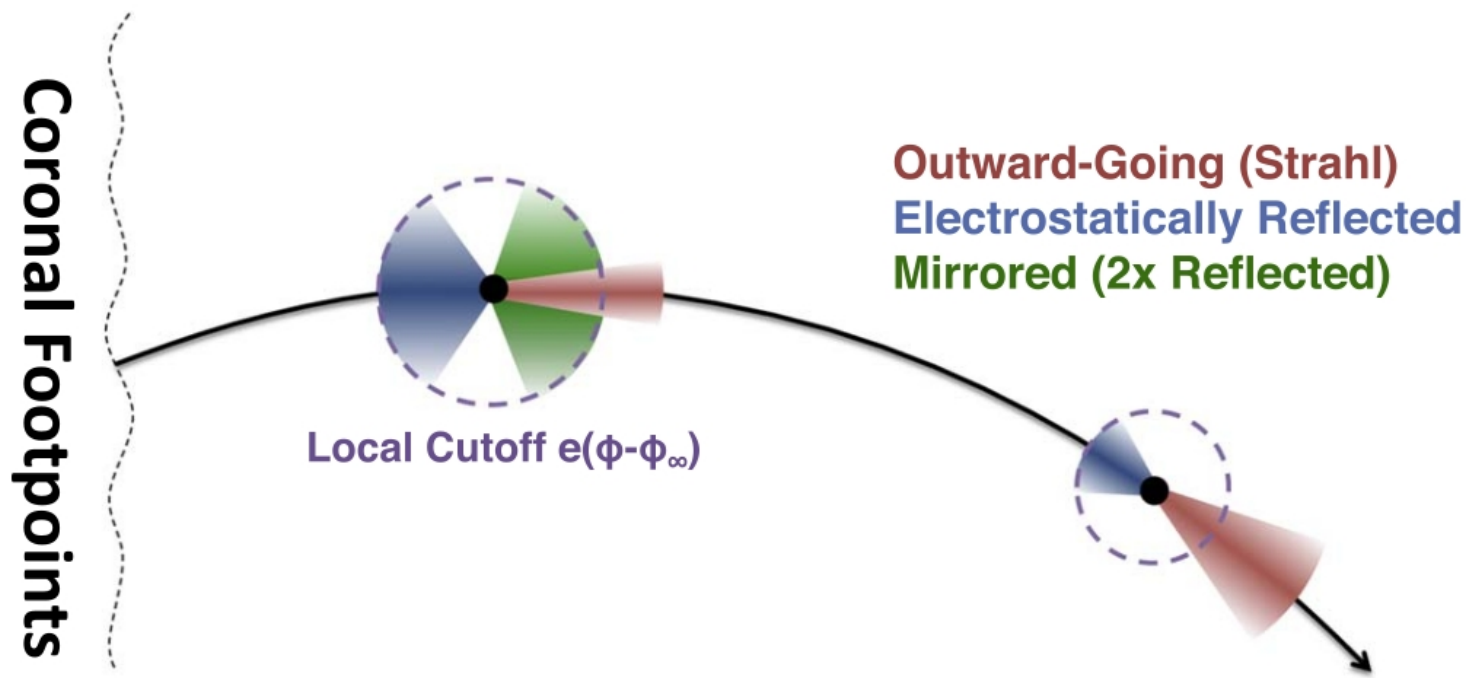


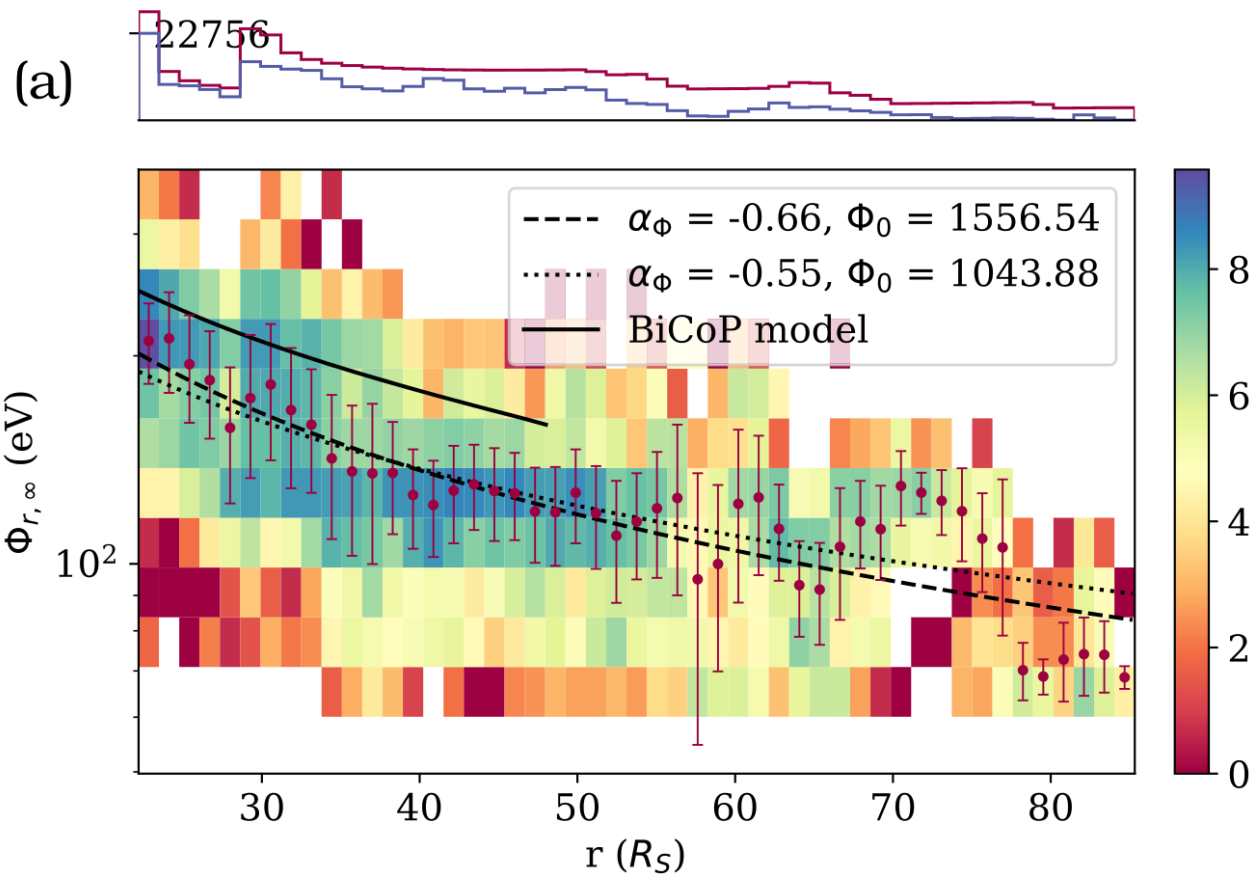
Image: Marc Pulupa

Core Deficit



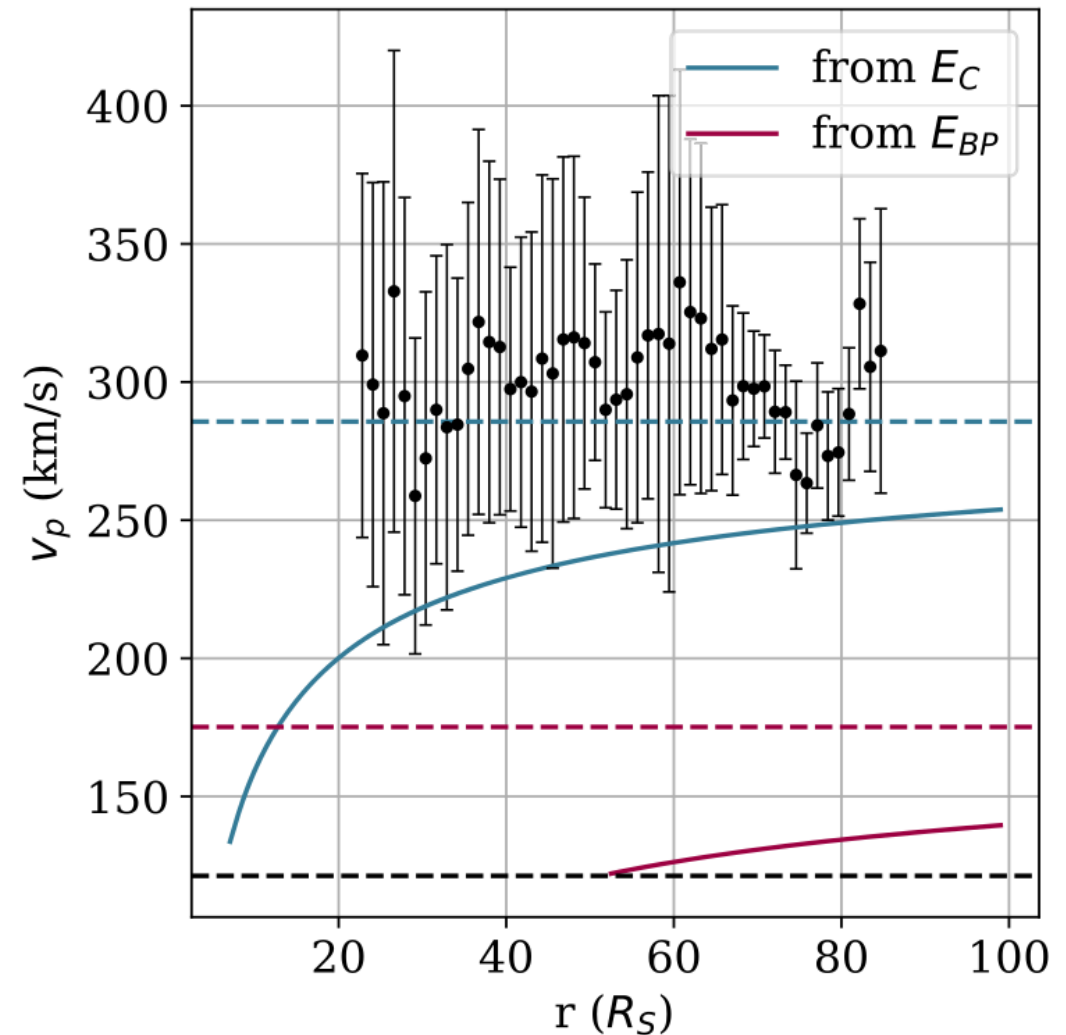
Halekas et al. (2021)

Core Deficit



Bercic et al. (2021)

Measurement of the core deficit (and breakpoint energy) provides estimate of ambipolar potential $20 R_s < r < 80 R_s$



Halo VDFs

Halo population:

- Suprathermal (100-1000 eV)
- Quasi-isotropic
- non-Maxwellian

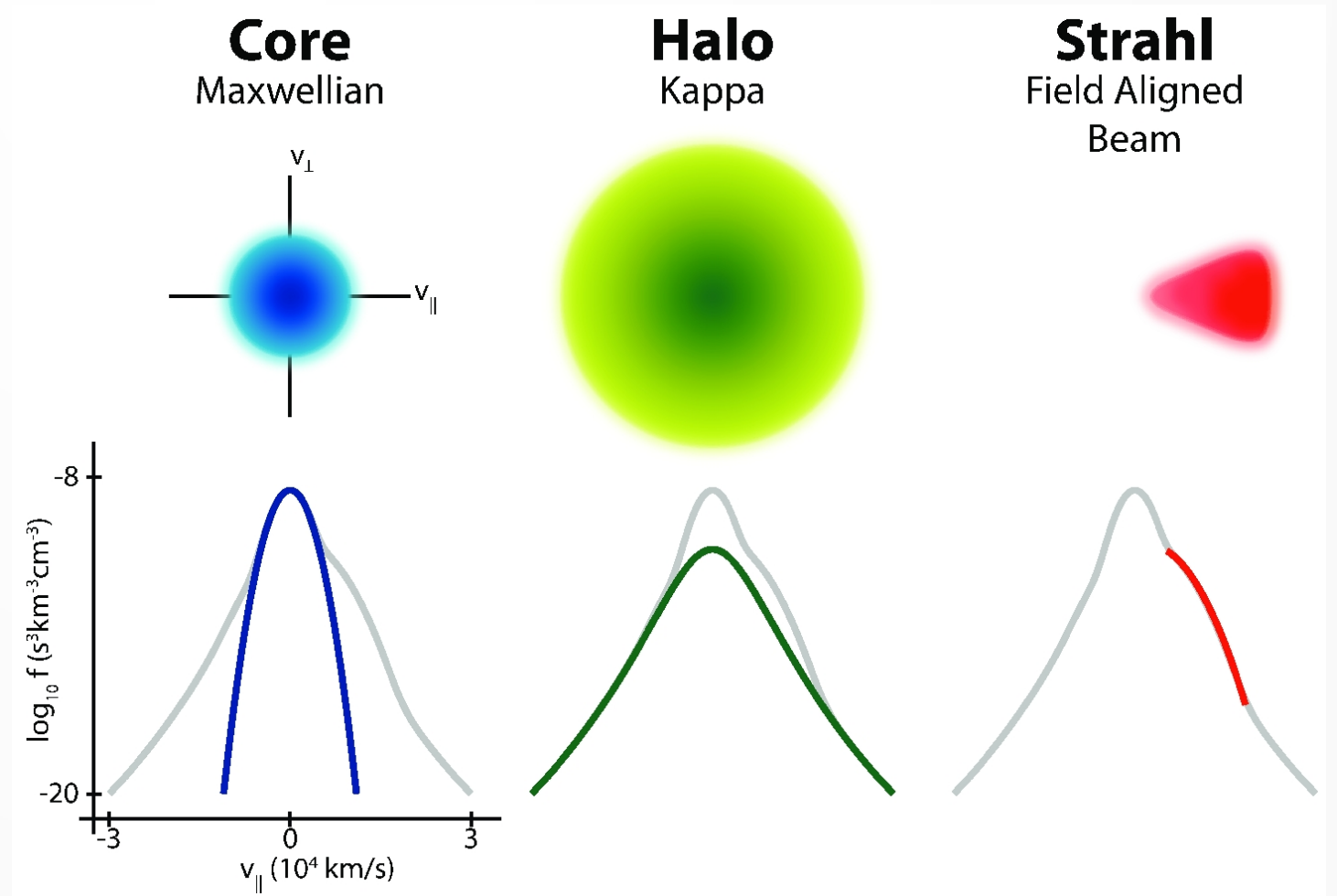
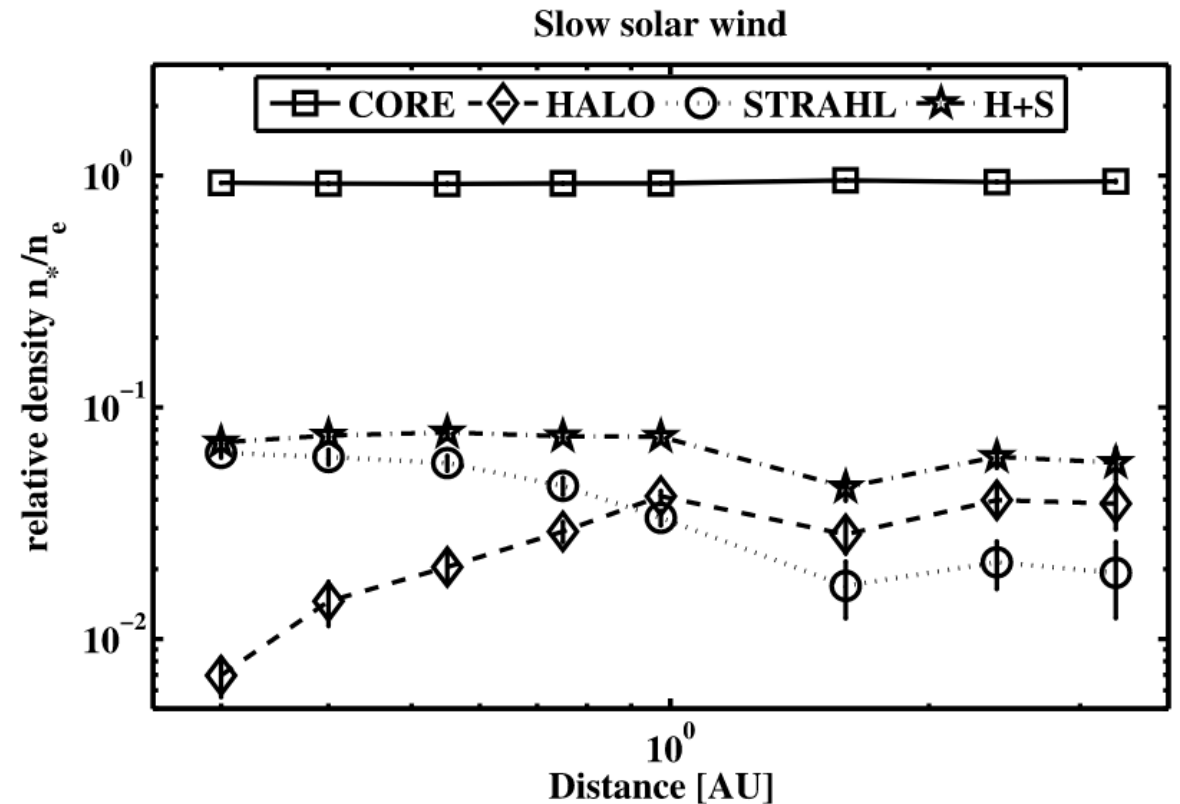
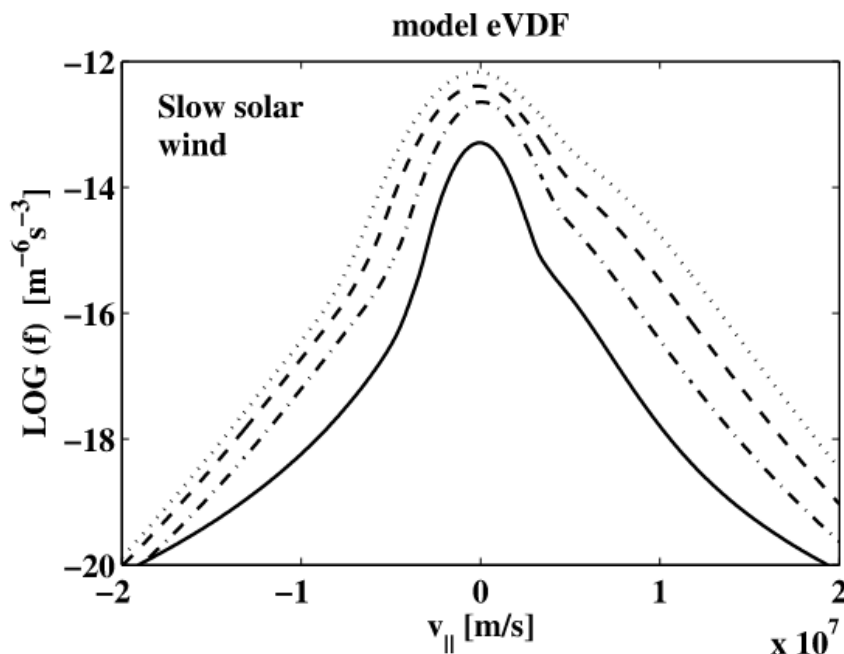


Image: Marc Pulupa

Halo VDFs

- A model of the halo needs to explain:
 - Energy spectrum
 - Isotropy
 - Evolution with distance

Stverak (2009)



Halo Origin

- Conventionally, the halo is formed from **local** wave-particle scattering of the strahl electrons
- Whistler waves
 - Kinetic Instabilities
 - Sub-proton scale turbulence

Whistler waves

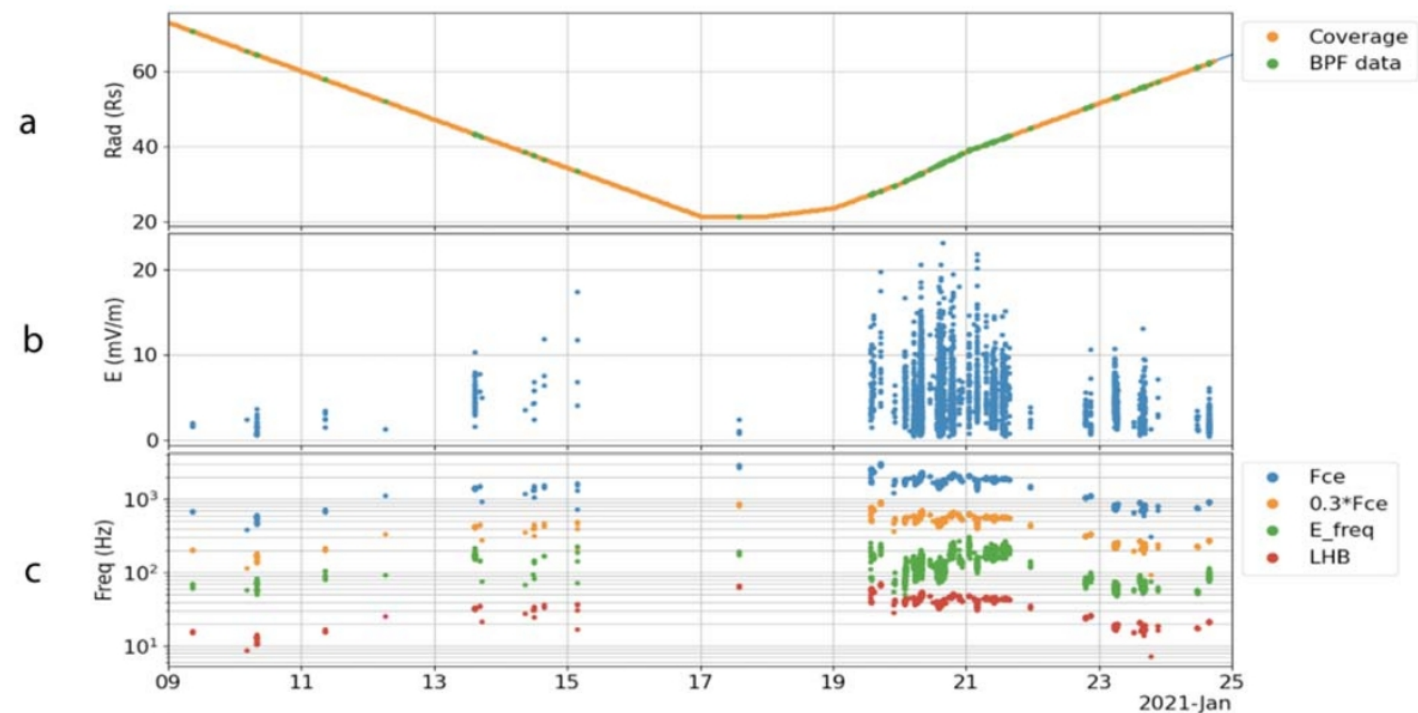
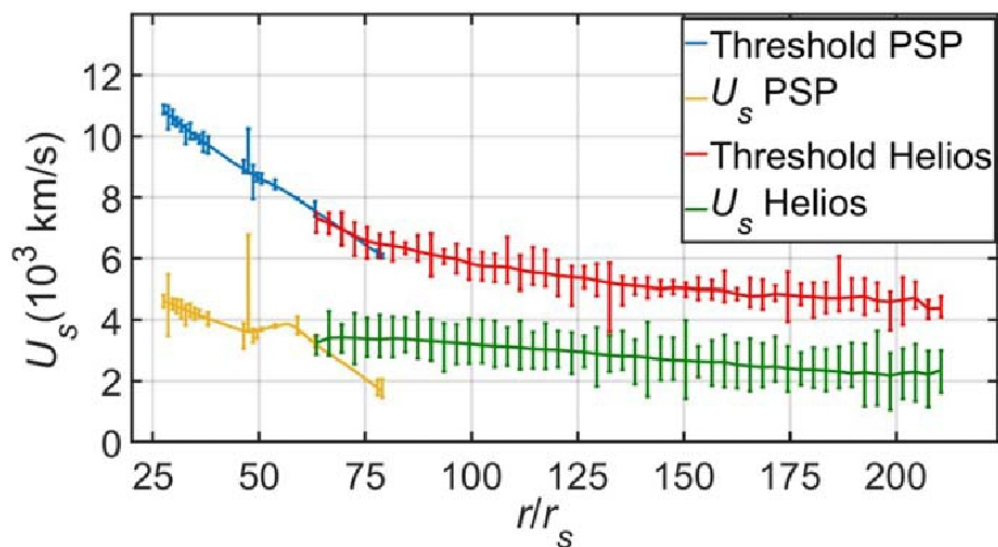
- Instabilities

- eVDF stable to Fast-magnetosonic/whistler waves

Jeong et al. (2022)

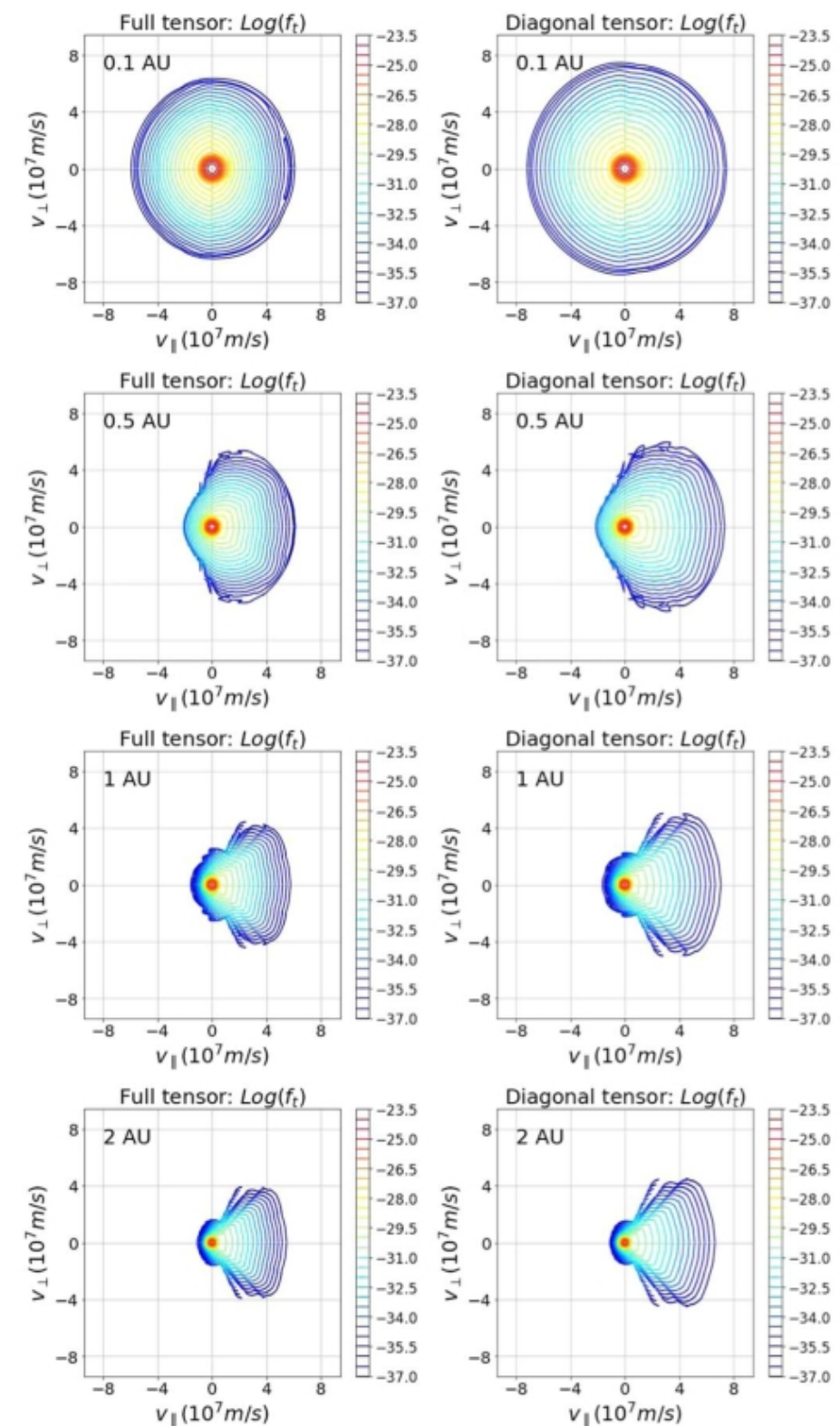
- No whistlers detected <28 solar radii (and intermittent elsewhere)

Cattell et al. (2022)



Whistler waves

- Turbulence
 - Tang (2022)
 - Applied quasilinear diffusion tensor to eVDFs
 - Critique: halo becomes less prominent with distance in the simulations
 - Boldyrev & Horaites (2019)
 - Whistler turbulence (if it exists) should be more relevant in the outer heliosphere
- Both these models require significant assumptions (e.g. spectral index)

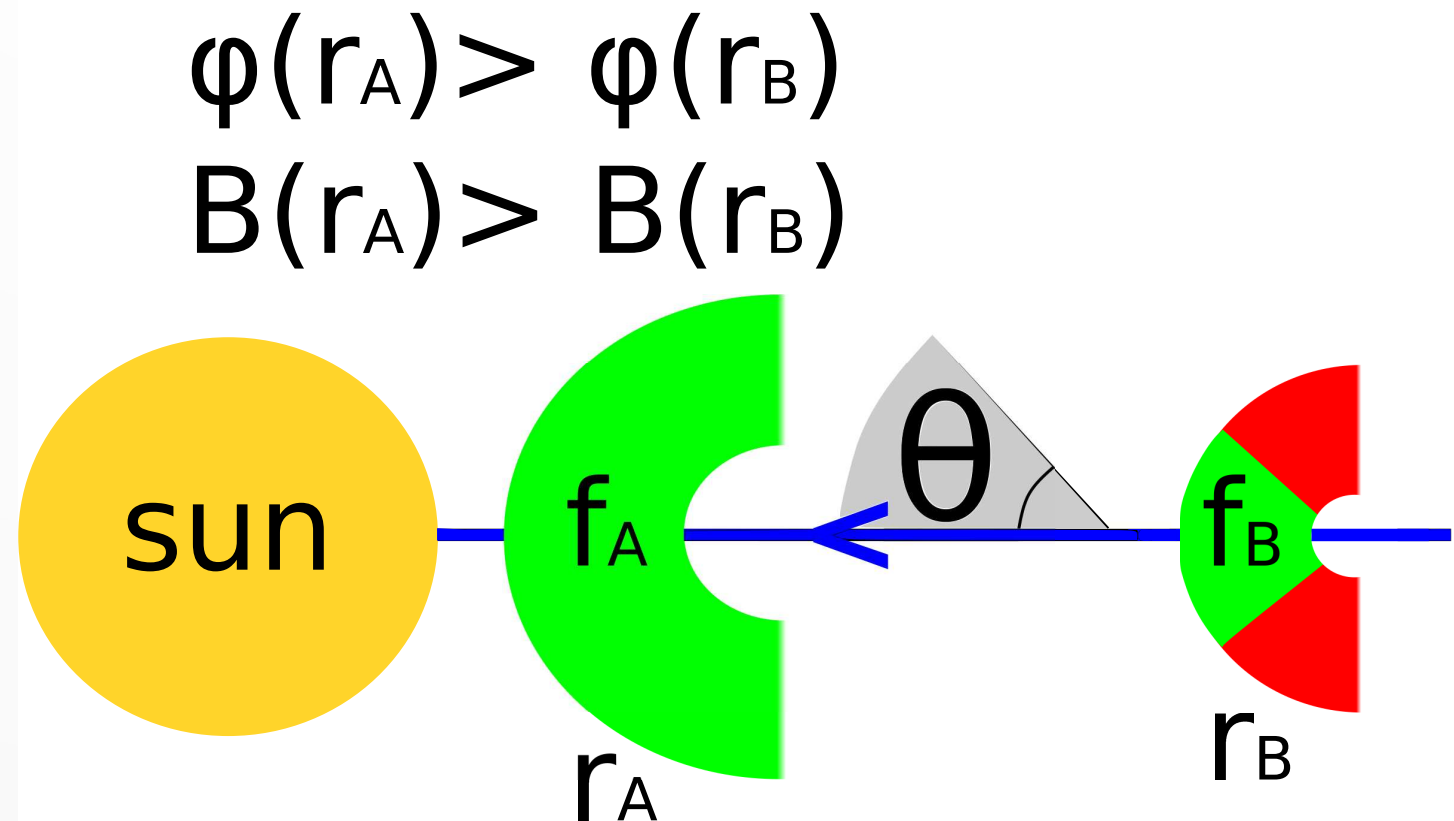


Scatter-Free Halo

- Halo observations have not yet been matched to a theory based on local scattering
- However, theory and observations agree there is a spatially-varying ambipolar potential (100-1000 eV)
 - Potential should dramatically affect the collisionless halo electrons (also 100-1000 eV).
- **Neglect** scattering. Such a model can explain:
 - Energy spectrum
 - Isotropy
 - Evolution with distance

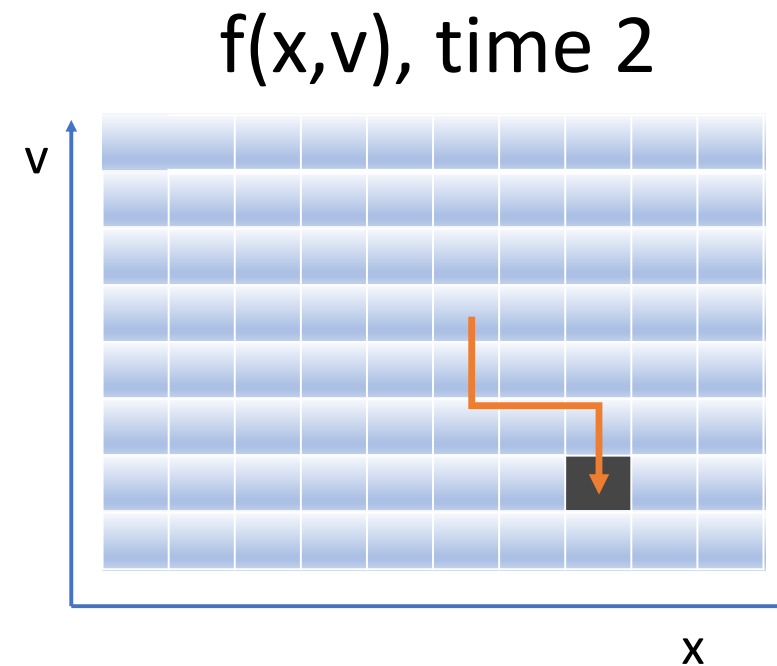
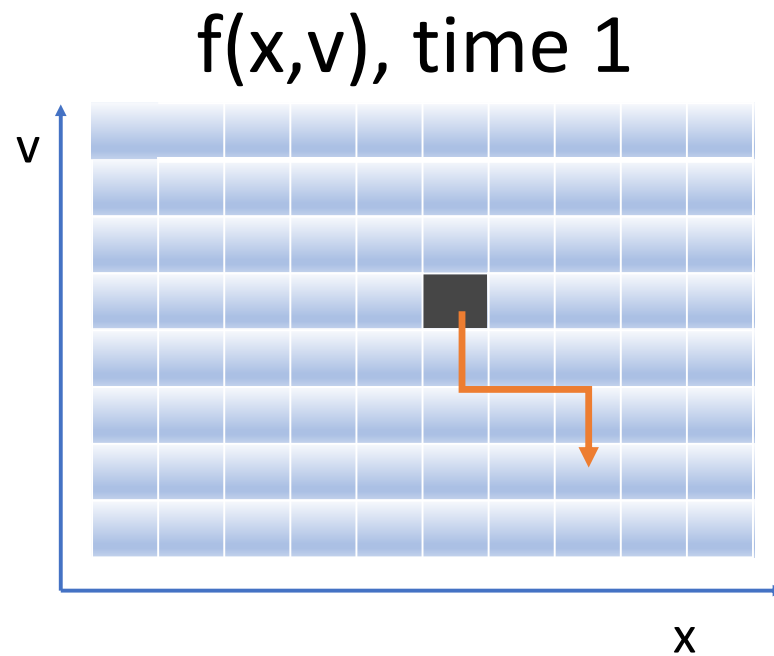
Collisionless model

- Assume **sunward-propagating** halo originates in the **outer** heliosphere
- Evolves collisionlessly in the inner heliosphere
- Consider eVDF evolution in the large scale fields
- Main effects:
 - Electric field
 - Magnetic mirroring



Liouville's theorem

Phase space density is **conserved** along particle trajectories in the **absence of diffusion**.



$$f(\mathbf{x}(t), \mathbf{v}(t), t) = f(\mathbf{x}_0, \mathbf{v}_0, t_0)$$

Liouville's theorem

In solar wind, collisionless electrons should conserve their total energy \mathcal{E} and magnetic moment M :

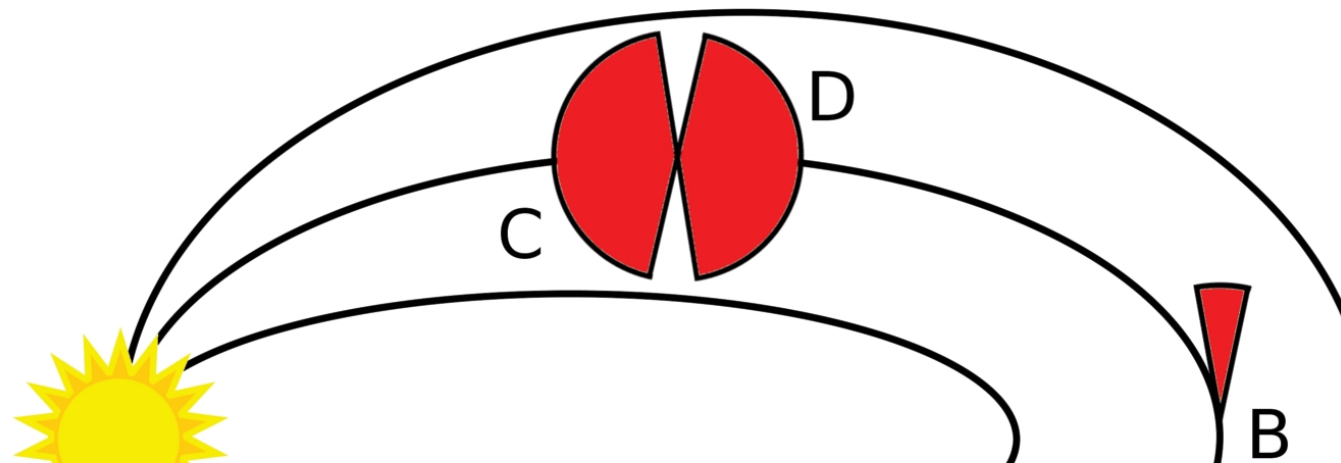
$$\mathcal{E} = K - e\phi(r)$$

$$M = \frac{K \sin^2 \theta}{B(r)}$$

As a consequence of Liouville's Theorem, steady-state distribution is simply a function of these conserved quantities:

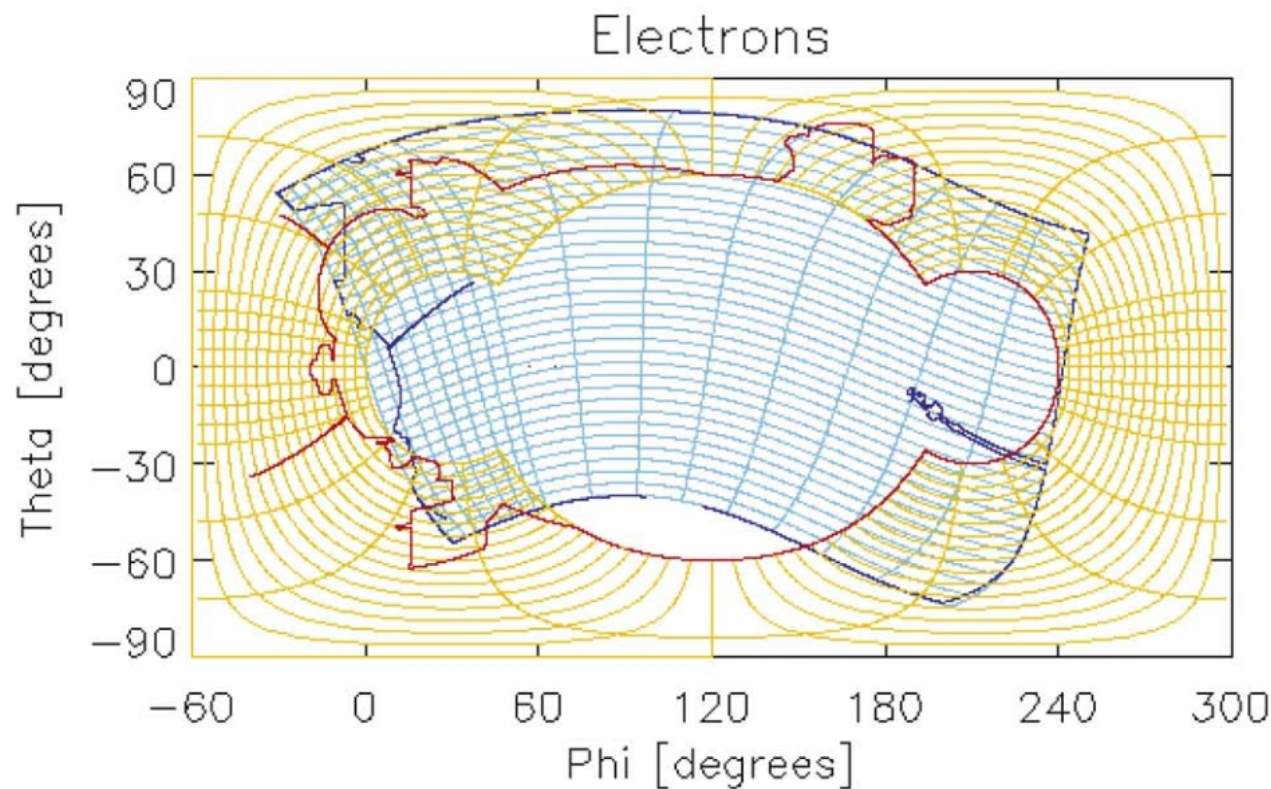
$$f = \tilde{f}(\mathcal{E}, M)$$

Horaites et al. (2019)

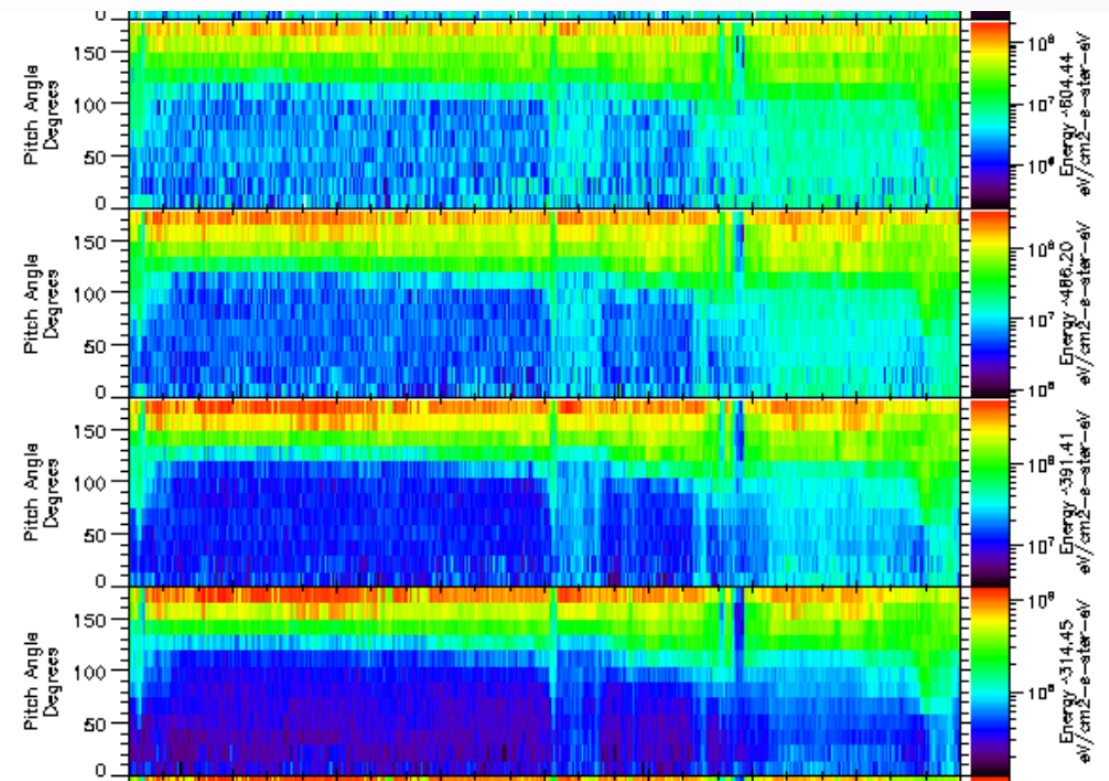


PSP SPAN-E Data

- Level 3 electron data
 - 2D Pitch angle distributions (32 energies, 16 angles)



Whittlesey et al. (2020)



CDAWeb PADs

Liouville's Theorem

Change variables (ignore time dependence):

K kinetic energy

θ pitch angle

$$f^\star(K, \theta) \equiv f(r_\star, K, \theta)$$

Boundary condition

$$f(r, K, \theta) =$$

“mapping” formula

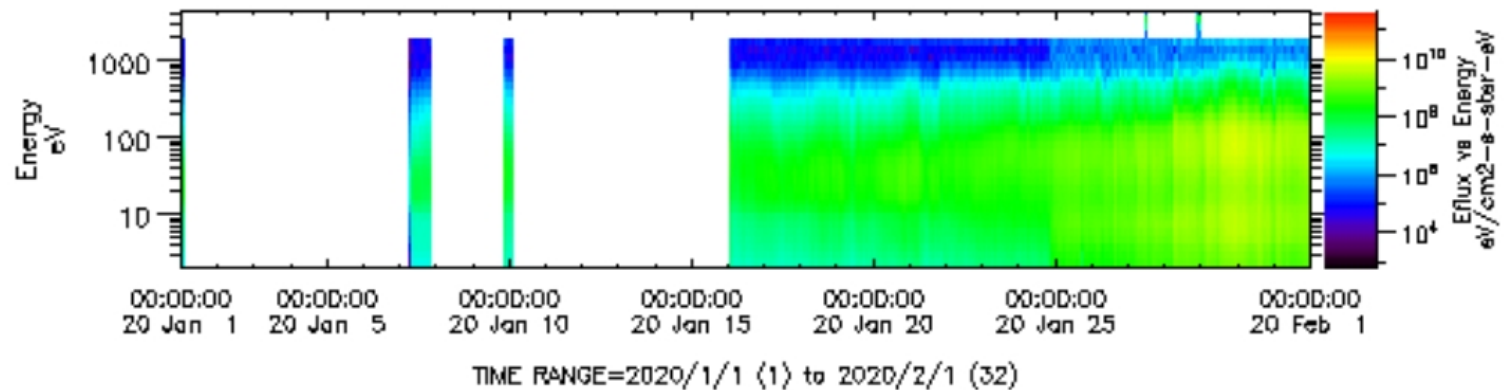
$$f^\star \left(K - e\Delta\phi(r, r_\star) , \sin^{-1} \sqrt{\frac{B(r_\star)K \sin^2 \theta}{B(r)(K - e\Delta\phi(r, r_\star))}} \right)$$

Liouville Mapping

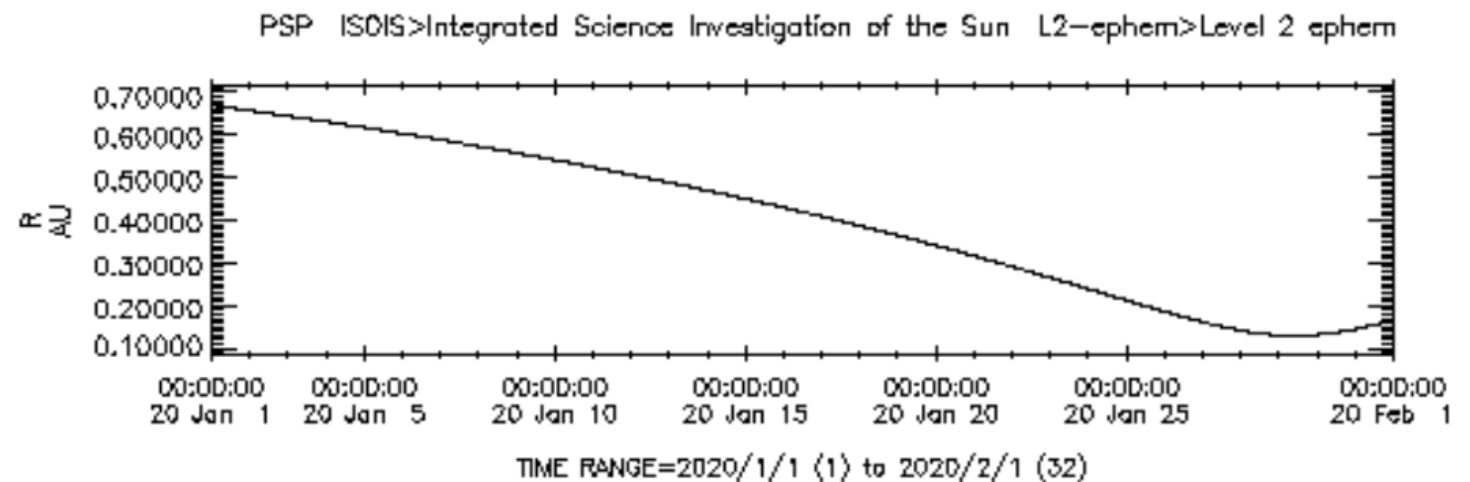
- Mapping formula depends on phase space variables r , K , θ , and the physical parameters $B(r)$, $\boldsymbol{\varphi}(\mathbf{r})$.
- Matching a function $f(r, K, \theta)$ consistent with Liouville's Theorem provides a **measurement** of the potential $\varphi(r)$.

SPAN-E PADs

- Want an overall picture of the eVDF evolution
- But data are sampled intermittently, at varying cadences
- To reduce bias, **average:**
 - In four hour intervals (decorrelation time)
 - By heliocentric distance (r)
- Time range:
 - 10/31/2018 to 12/31/2020
 - $0.2 \text{ AU} < r < 0.8 \text{ AU}$
 - >2 years around solar minimum, quiet conditions
 - Remove CMEs, CIRs, SIRs

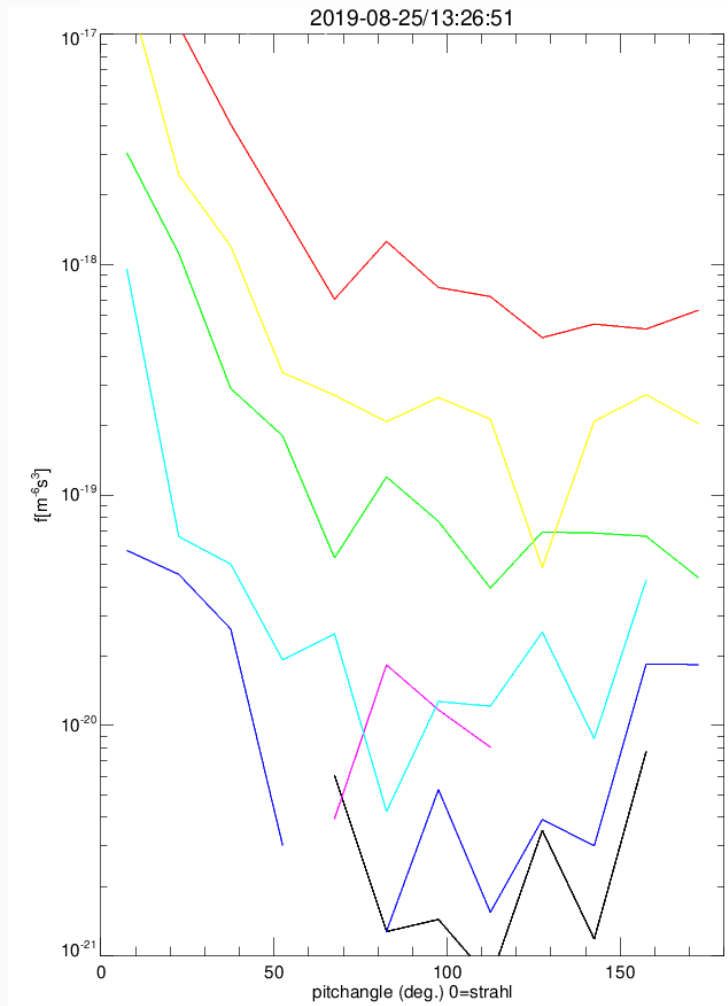


Total DEF (CDAWeb)

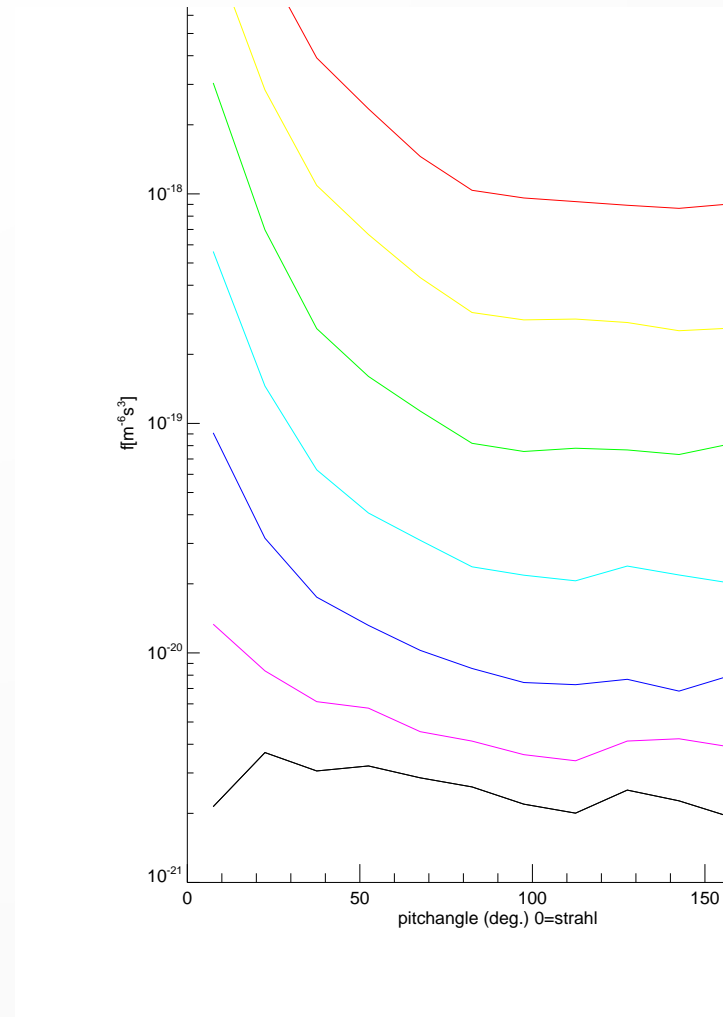


Heliocentric Distance (CDAWeb)

SPAN-E PADs (examples)

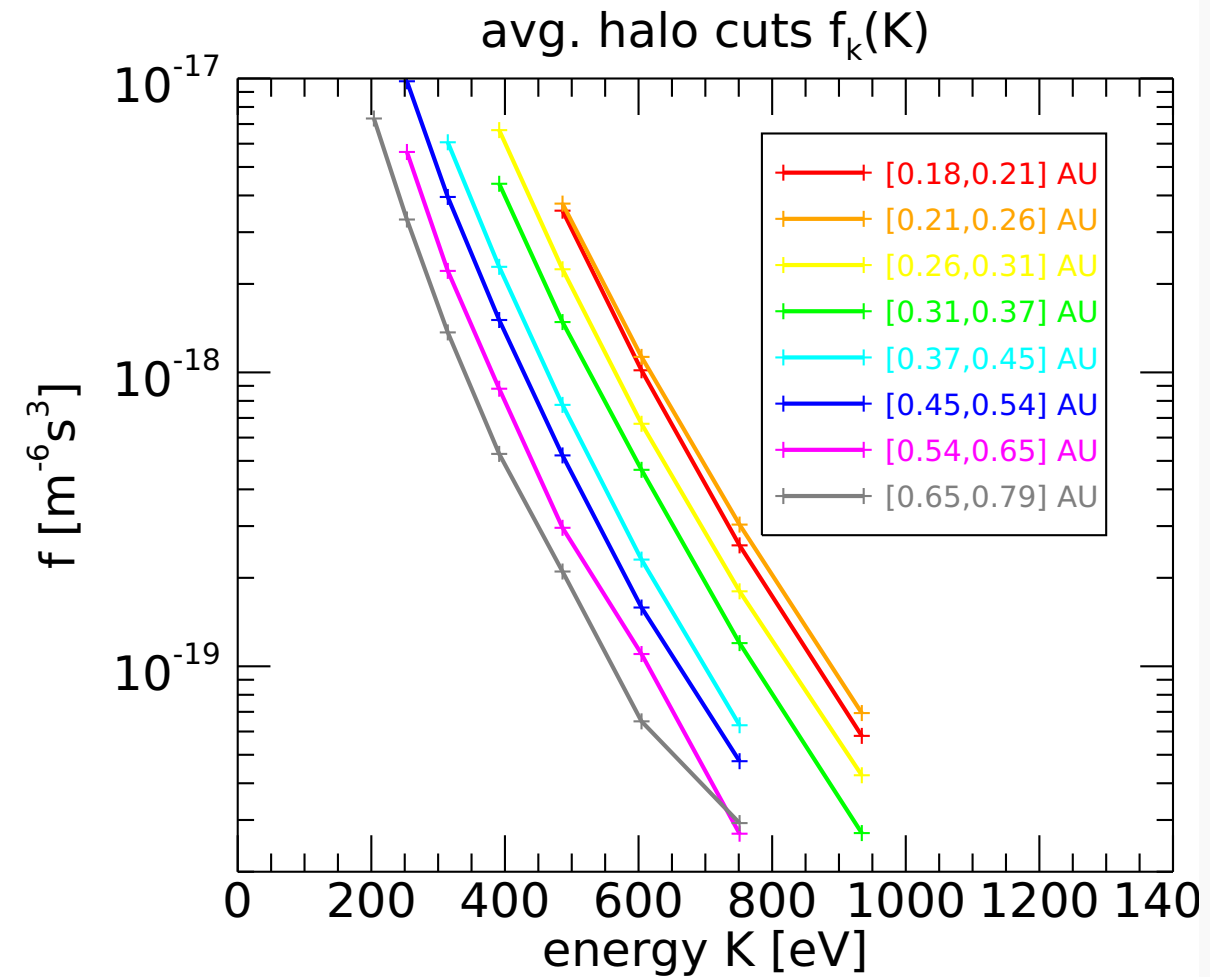
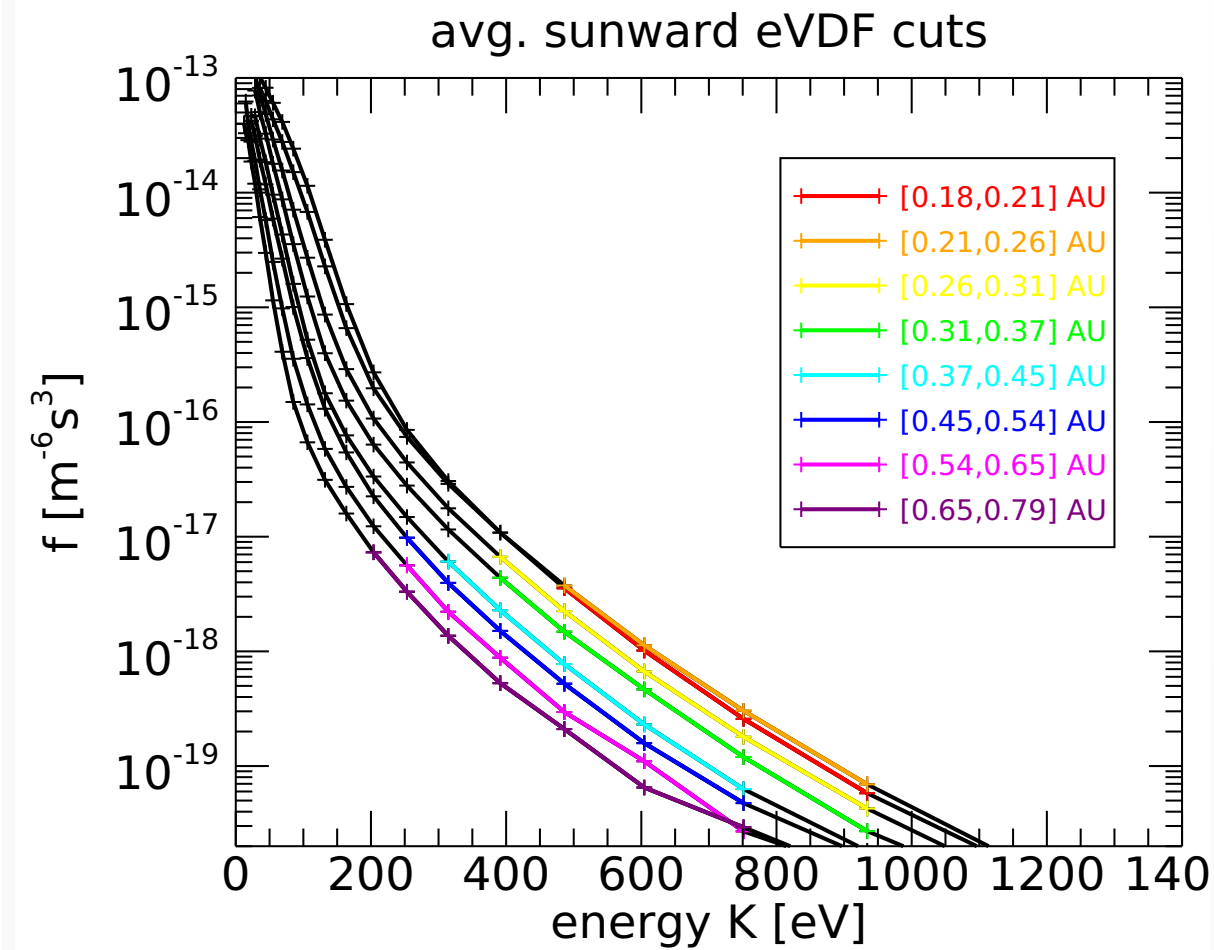


PAD (raw)



PAD (4-hour avg.)

Distance Average

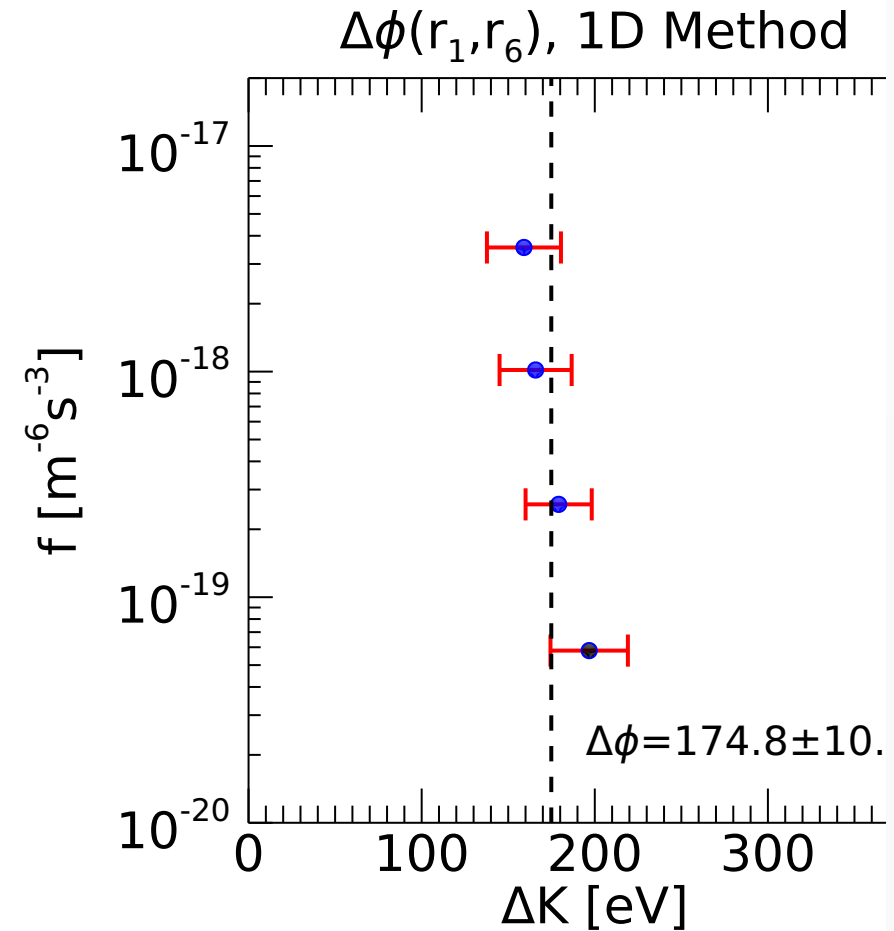
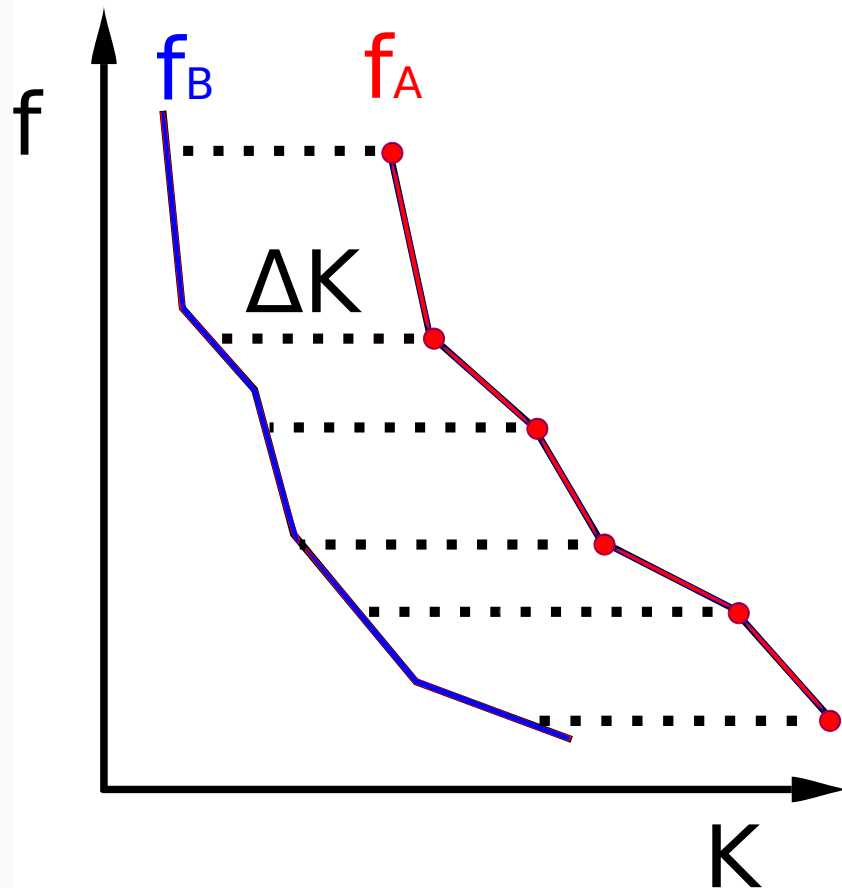


Sunward-propagating ($\theta=15$ deg.) cuts vs. distance

Liouville Mapping (1D)

1D mapping formula
(Special case $\theta=0$ deg.)

$$f_A(K) = f_B(K - e\Delta\phi(r_A, r_B))$$



Liouville Mapping (1D)

Results: 250 eV difference between
0.18 and 0.79 AU!

r range [AU]	1D Method: $\Delta\phi(r_1, r_k)$ [V]
[0.18, 0.21]	-0.00 \pm 0
[0.21, 0.26]	-18.9 \pm 23.2
[0.26, 0.31]	25.56 \pm 13.0
[0.31, 0.37]	63.26 \pm 13.2
[0.37, 0.45]	134.6 \pm 9.48
[0.45, 0.54]	174.8 \pm 10.4
[0.54, 0.65]	213.9 \pm 8.74
[0.65, 0.79]	250.7 \pm 7.80

Liouville Mapping (2D)

Assume a boundary condition can be matched to a 2D polynomial in θ , K :

$$\ln f^\star(K, \theta) = \ln f(r_N, K, \theta) = \sum_{i=0}^D \sum_{j=0}^D A_{ij} \theta^i K^j$$

$$f(r, K, \theta) =$$

$$f^\star \left(K - e\Delta\phi(r, r_\star), \sin^{-1} \sqrt{\frac{B(r_\star)K \sin^2 \theta}{B(r)(K - e\Delta\phi(r, r_\star))}} \right)$$

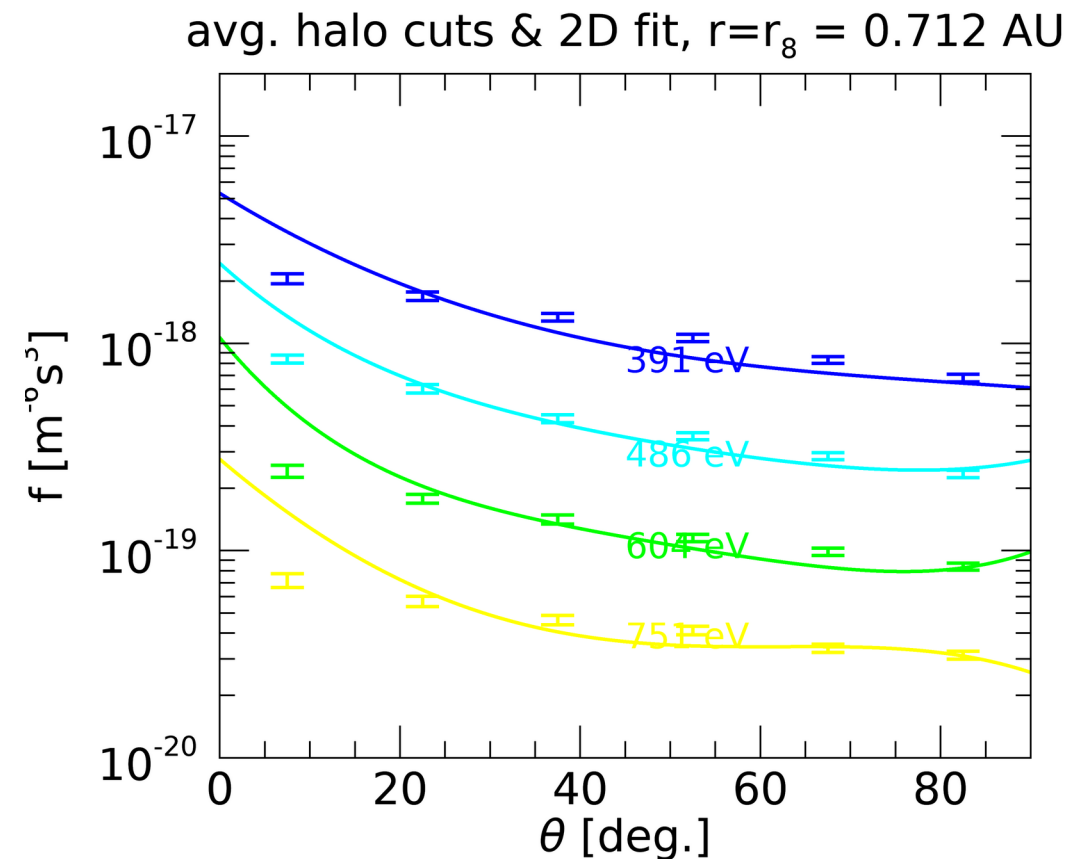
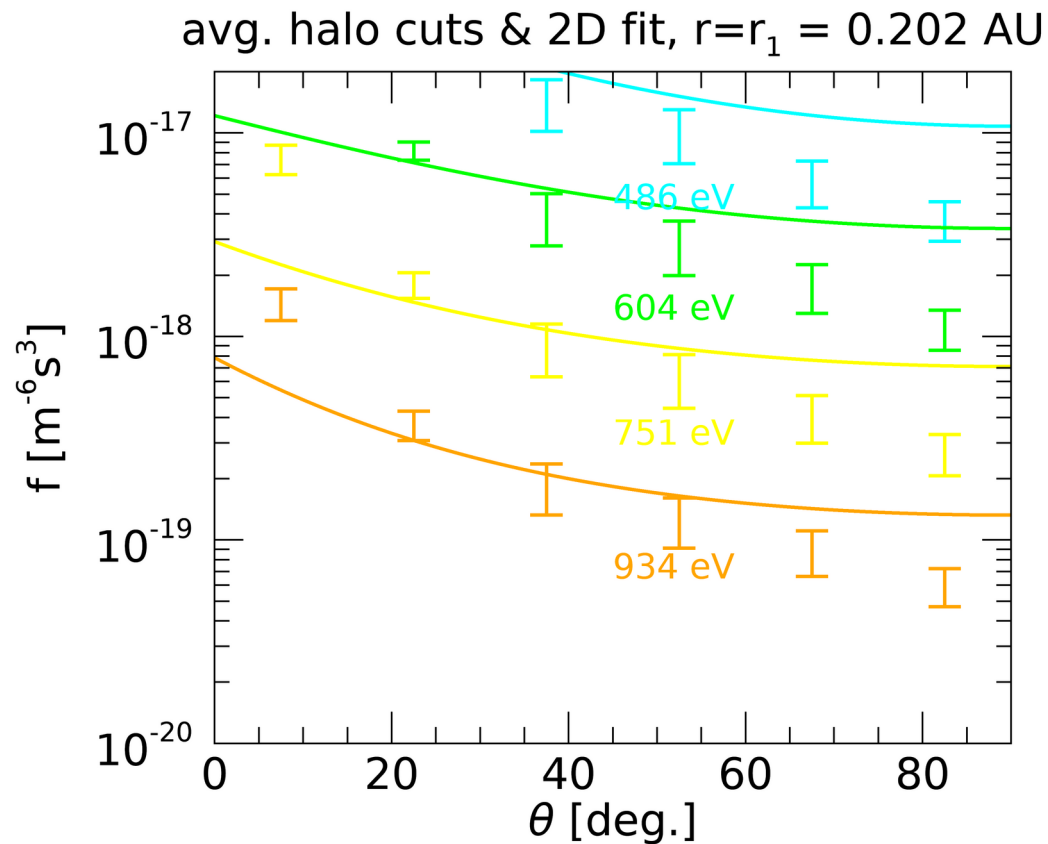
Liouville Mapping (2D)

- Fitting to the 2D function matches data at all observed distances
- Confirms that Liouville's theorem applies to the data
- Similar potentials as 1D method

Validation (Strahl)

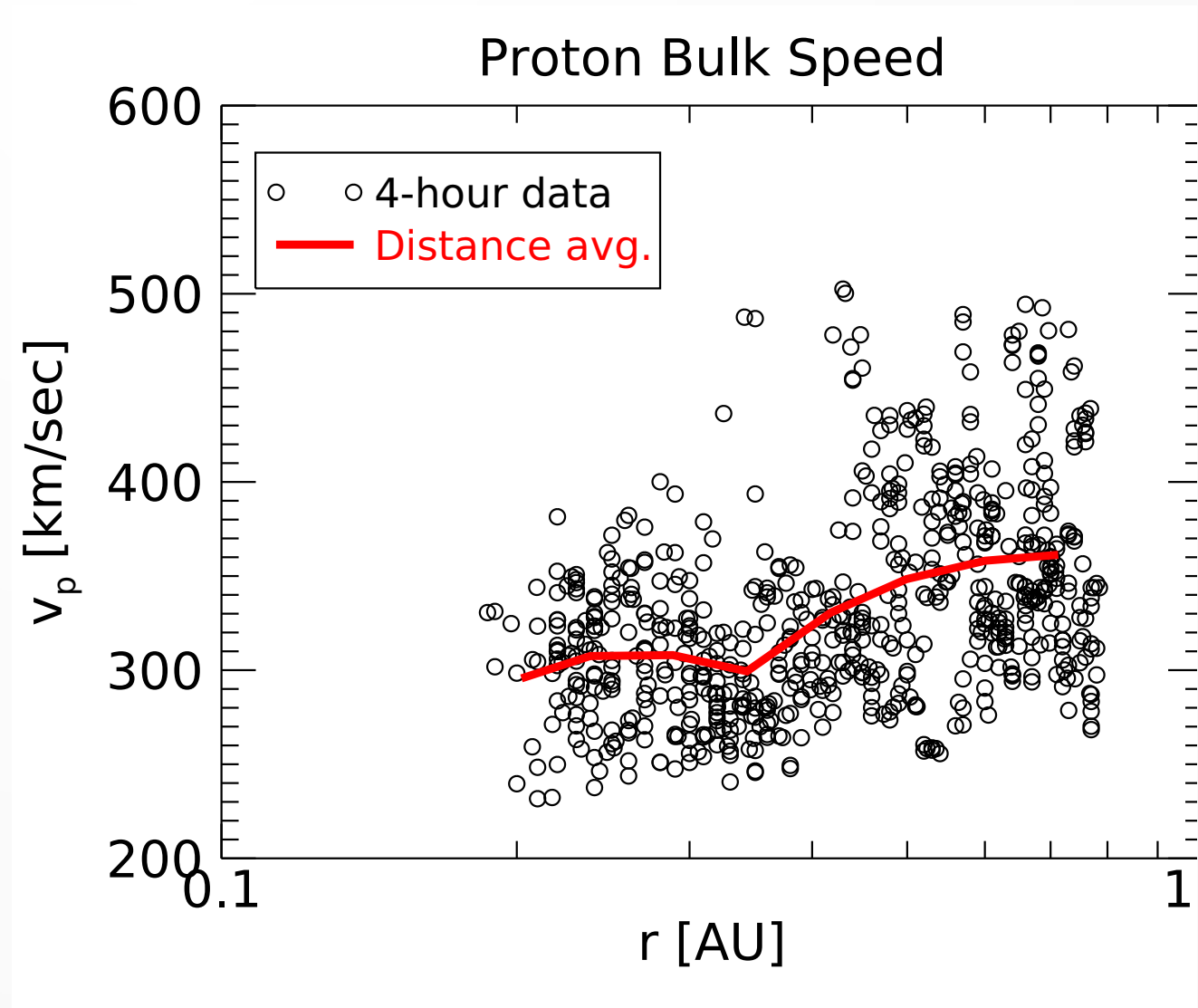
- Liouville's theorem can't match arbitrary data
- Liouville mapping the strahl fails
- Scattering must affect the strahl, but halo may be scatter-free

Strahl data:



Solar wind acceleration

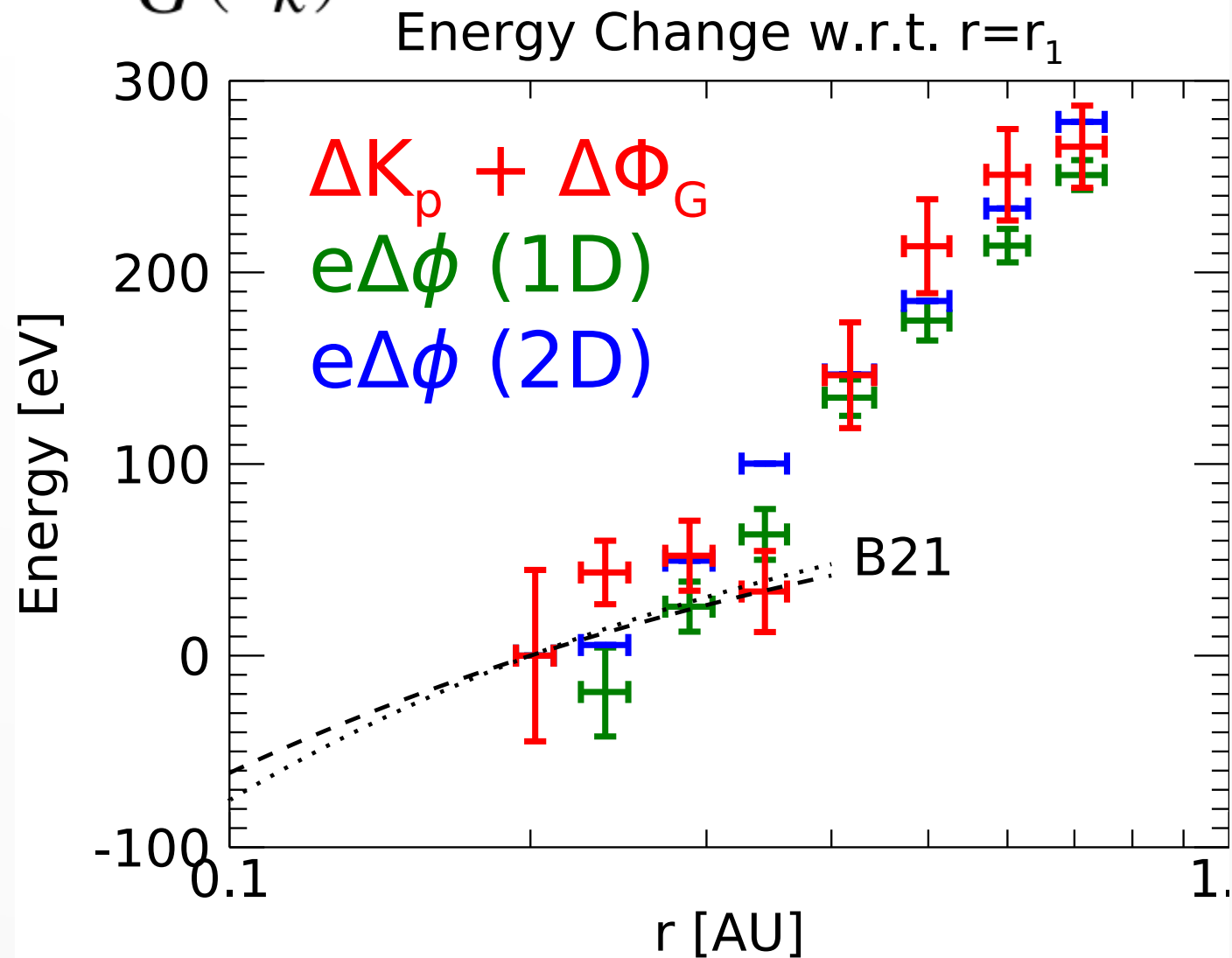
- Faraday cup data (fit to radial velocity component)
- 4-hour averages
- Protons accelerate from 290 km/sec to 360 km/sec (230 eV increase in kinetic energy)



Ambipolar Potential

$$e\Delta\phi(r_1, r_k) = \Delta K_p(r_k) + \Delta\Phi_G(r_k)$$

- Correct total proton energy by gravity
(~ 40 eV correction)
- Both measurements of potential agree
(electrons and protons)
- The same potential must be responsible for the observed electron and proton signatures



Conclusions

- Evolution of sunward-propagating halo is consistent with Liouville's theorem
- Scatter-free assumption allows calculation of the ambipolar potential
- Inferred potential consistent with the observed proton acceleration
- Evolution of the halo in the inner heliosphere fully explained
 - *Still require a source of sunward-propagating halo electrons in the outer heliosphere